

Physiological and molecular mechanisms of radicle development of somatic embryos in *Schisandra chinensis* cultured in the dark

DAN SUN

sundan@jlau.edu.cn

Jilin Agricultural University

SU Zhang

Jilin Agricultural University

jun Ai

Jilin Agricultural University

Zhenxin Wang

Jilin Agricultural University

Guangli Shi

Jilin Agricultural University

Jianhui Guo

Jilin Agricultural University

XIN Song

Jilin Agricultural University

Meng Li

Jilin Agricultural University

Yunqing Liu


Jilin Agricultural University

Research Article

Keywords: *Schisandra chinensis*, Somatic embryo, Radicle, Plant hormone, Gene expression

Posted Date: November 10th, 2023

DOI: <https://doi.org/10.21203/rs.3.rs-3555472/v1>

License:  This work is licensed under a Creative Commons Attribution 4.0 International License. [Read Full License](#)

Version of Record: A version of this preprint was published at Plant Cell, Tissue and Organ Culture (PCTOC) on March 18th, 2024. See the published version at <https://doi.org/10.1007/s11240-023-02662-9>.

Abstract

Somatic embryogenesis (SE) is a method for producing plant embryos in vitro and is considered a highly promising approach for micropropagation. As a valuable Chinese herbal medicine, the application of SE in genetic breeding, such as in *Schisandra chinensis*, faces several technical challenges, including incomplete development of somatic embryos and difficulties in plant regeneration. Here, we established an efficient plant regeneration pathway for somatic embryos in *S. chinensis*. In this experiment, dark culture conditions were found to significantly improve the plant regeneration rooting rate through SE. To understand the genetic mechanism governing embryogenesis, a comparative transcriptome analysis was performed to elucidate differences between light and dark conditions on somatic embryo development in *S. chinensis*. Dormant buds of *S. chinensis* were used as explants, and embryonic calli were cultured in light (16 h/D) or dark conditions for 28 days. The cultivation of explants in darkness has been shown to significantly enhance the production of somatic embryo radicles. Under dark conditions, radicle primordia were initiated at the globular embryo stage and developed from the heart-shaped to the torpedo-shaped embryo stages. To explore the *S. chinensis* root mechanism, endogenous hormones were quantified, and RNA-seq analysis was performed throughout the process of somatic embryogenesis. The results indicated that from the globular to heart-shaped embryo stages, the levels of IAA and ABA in somatic embryos subjected to the dark treatment were markedly lower ($190.965 \text{ ng}\cdot\text{g}^{-1}$ and $525.152 \text{ ng}\cdot\text{g}^{-1}$) than those in somatic embryos exposed to light ($597.565 \text{ ng}\cdot\text{g}^{-1}$ and $749.188 \text{ ng}\cdot\text{g}^{-1}$), while the concentrations of GA_3 and ZR were lower at all stages under light treatment. Transcriptome sequencing and bioinformatics analysis revealed that the pathways and processes in which the differentially expressed genes in somatic embryos under dark conditions were predominantly enriched were plant hormone signaling, circadian rhythm, and phenylpropanoid biosynthesis. qRT-PCR was employed to validate the expression of plant hormone signaling transduction-related genes, including *GH3*, *SAUR*, *ARF1*, *ARF18*, *AUX/IAA*, *MMK1*, *AHK4*, *AHK5*, and *PIF3*, and the results were consistent with the transcriptome sequencing results. This work laid the foundation for applied research and could be useful in future reluctant woody plant improvement programs and can even be extended to other species.

Key Message

Dark culture significantly improved the radicle development of somatic embryos in *S. chinensis* and the differentially expressed genes were predominantly enriched in plant hormone signals, which corresponded to endogenous hormone levels.

Introduction

Schisandra chinensis (Turcz.) Baill. is a deciduous woody vine plant of the *Schisandraceae* family that is mainly distributed across Northeast China, the Korean Peninsula and the far east of Russia (Ai et al. 2012), which has a broad market and offers significant economic and medicinal value (Ye et al. 2019). The dried fruit of *S. chinensis* has been a valuable Chinese herbal medicine for thousands of years and contains hundreds of compounds, including lignans, triterpenoids, flavonoids, and tannins (Liu et al. 2023). These compounds exhibit various pharmacological effects, such as anti-inflammatory, hypnotic, antiasthmatic, and hepatoprotective effects, in addition to having preventive effects against Alzheimer's disease. Additionally, *S.*

chinensis compounds enhance the sensitivity of anticancer drugs and exhibit anti-human immunodeficiency virus (HIV) activities, as well as effects on physical performance and the central nervous system (Bai et al., 2015; Xu et al., 2015; Chen et al., 2019; Song et al. 2021). Apart from its medicinal use, *S. chinensis* can also be utilized to produce fruit wine, jam, juice drinks, and health care products, indicating its broad market application prospects (Ai et al. 2022). As a traditional tonic herb and food, the annual demand for *S. chinensis* is more than 30,000 tons. Due to the immaturity of asexual reproduction technology, the cultivation of *S. chinensis* is mostly based on seedling cultivation, which greatly hinders the process of variety development (Sun et al. 2020).

Somatic embryo regeneration is the process by which somatic cells undergo morphogenesis to form complete plants via a developmental pathway similar to that of sexual zygotic embryos, without the fusion of germ cells (Fehér 2015). Plant somatic embryos possess the same totipotency as zygotic embryos and can be induced under appropriate culture conditions (Xu et al. 2019). The genetic variability of somatic embryos is relatively stable, with less variability than occurs in regenerated plants formed through organogenesis (Duclercq et al. 2011). Somatic embryogenesis is a superior method for breeding excellent cultivars and conserving resources. Unlike organogenesis, somatic embryos exhibit polarity in the radicle and germ at the early stages. Numerous studies have demonstrated successful regeneration of plants through somatic embryogenesis. However, several factors influence the establishment of the regeneration system. Many experiments have shown that different light conditions play a crucial role in the induction of calli, as well as in the development and maturation of embryoids during somatic embryogenesis (Yuan et al. 2003).

S. chinensis exhibits a low rooting rate during conventional vegetative propagation (Li 2012). To overcome this bottleneck, we investigated the effects of different light treatments on somatic embryo rooting in this species in the current study. In this study, we elucidated the physiological and molecular mechanisms underlying primary root development in this species by examining the morphological structure of the *S. chinensis* somatic embryo radicle, analyzing the dynamic changes in the radicle endogenous hormone content, and identifying the differentially expressed genes in the radicle. Our findings have significant implications for the large-scale production of seedlings and provide valuable insights for improving plant asexual reproduction techniques.

Materials and methods

Plant materials

The dormant buds of the 'Zaohong' cultivar were collected from the *S. chinensis* germplasm repository at Jilin Agricultural University (43°48'005"N, 125°24'15"E) in Changchun City, Jilin, China. Callus was induced from the buds on embryogenic callus medium (MS + 2,4-D 3.0 mg·L⁻¹ + sucrose 30 g·L⁻¹ + agar 6.5 g·L⁻¹) (MS, sucrose and agar were from Chembase, Shanghai, China; 2,4-D was from Sigma, Darmstadt, Germany) under a light intensity of 25 μmol·m⁻²·s⁻¹ for 16 h/d. The embryogenic calli were then cultured on medium (1/3 MS + 20 g·L⁻¹ sucrose and 6.5 g·L⁻¹ agar) under light (25 μmol·m⁻²·s⁻¹, 16 h/d) or dark conditions for somatic embryogenesis. The samples obtained during the embryonic callus stage were labeled as the control (CK); those obtained under light conditions at 7, 14, 21, and 28 days of culture were labeled GZ1, GZ2, GZ3, and GZ4, and those collected under dark conditions at 7, 14, 21, and 28 days of culture were labeled HA1, HA2, HA3, and HA4. Three samples per group were selected for measurement at each period to establish three

replicates. The fresh weight of each sample to be tested was greater than 0.5 g, and the samples were stored at -80°C after collection.

Paraffin section preparation

The observation of plant tissue structure was conducted using the paraffin section method described by Wang (2010). Somatic embryos at various developmental stages were collected, washed, fixed in formalin–acetic acid–alcohol (FAA) (Coolaber, Beijing, China), dehydrated using a tert-butyl alcohol gradient (TBA) (Sinopharm, Beijing, China), and embedded in wax. The samples were then sliced into 10–12 µm sections using a rotary slicer, stained with safranin-fast green (Solarbio, Beijing, China), and sealed with Canadian gum (Sigma, Darmstadt, Germany). Microscopic observation and photography were performed using a Nikon Eclipse Ti-S.

Determination of endogenous hormone contents

IAA, ZR, ABA and GA₃ were determined by enzyme-linked immunosorbent assay (ELISA). The ELISA kit and extraction method were provided by China Agricultural University.

RNA-Seq analysis

RNA extraction, library preparation and sequencing were performed by Lianchuan Biological Co., Ltd. All assembled unigenes were aligned against the nonredundant (Nr) protein database (<http://www.ncbi.nlm.nih.gov/>), Gene Ontology (GO) (<http://www.geneontology.org/>), SwissProt (<http://www.ExPASy.ch/sprot/>), Kyoto Encyclopedia of Genes and Genomes (KEGG) (<http://www.genome.jp/kegg/>) and eggNOG (<http://eggnogdb.embl.de/>) databases using DIAMOND (Buchfink et al., 2015) with a threshold of Evalue < 0.00001.

Differentially expressed Unigene analysis

The Salmon tool (Patro et al. 2017) was used to determine the expression level of Unigenes by calculating transcripts per kilobase million (TPM) (Mortazavi et al. 2008). The differentially expressed Unigenes were selected with log₂ (fold change) > 1 or log₂ (fold change) < -1 and with statistical significance (p value < 0.05) by R package edgeR (Robinson et al. 2010).

qRT-PCR verification

The genes *GH3*, *SAUR*, *ARF1*, *ARF18*, *AUX/IAA*, *MMK1*, *AHK4*, *AHK5*, and *PIF3* were selected to investigate expression patterns under light and dark conditions. The primers were synthesized by Shanghai Shengggong Biological Co., Ltd. (Table 1). RNA was reverse transcribed into cDNA using a TaKaRa reverse transcription kit, and quantitative PCR was performed using TB Greenpremix Ex Taq (TaKaRa, Dalian, China) with *AcTIN* as the reference gene. The reaction mixture consisted of 10 µl, 0.4 µl of upstream and downstream primers, 5 µl of TB Green, 1 µl of cDNA template, 0.2 µl of ROX, and 3 µl of ddH₂O. The reaction was carried out at 95°C for 35 minutes, 60°C for 30 minutes, and 95°C for 15 minutes. Then, the process was repeated three times for each sample sitting at 60°C for one hour. The relative expression was calculated using the 2^{-ΔΔCT} method.

Table 1
Lists of qRT-PCR primers

Gene ID	Gene name		Primer sequence (5'-3')
TRINITY_DN23647_c0_g4	<i>AcTIN</i>	Forward (5'-3')	GAAGCACTTTCGGTGGACAA
		Reverse (5'-3')	GGGGTGCTATACTAGCCAAA
TRINITY_DN29853_c1_g7	<i>GH3</i>	Forward (5'-3')	AGCCGCCAAGATTGAAAGGACTA
		Reverse (5'-3')	GAGCAACAGACGCCAGGAAGCAA
TRINITY_DN31702_c2_g4	<i>SAUR</i>	Forward (5'-3')	TTACCCGCCGACCATTTCTATTT
		Reverse (5'-3')	CCTCAACCTCTTCCGTTTCGTCTT
TRINITY_DN25935_c0_g1	<i>ARF1</i>	Forward (5'-3')	ACCACTACGACCACCTTTCTAAT
		Reverse (5'-3')	GAAACAGTAACTGGGTTGTGAGA
TRINITY_DN26635_c0_g6_i1	<i>ARF18</i>	Forward (5'-3')	AGTTGCTCCCGTTGAAGGATTTGG
		Reverse (5'-3')	CCTCCACATCAAGACCACTGCTATC
TRINITY_DN20787_c1_g3	<i>AUX/IAA</i>	Forward (5'-3')	ATGAAGAGTTGGAGCCATGAAGT
		Reverse (5'-3')	TGTATAACCAGGAGCCAAATGAG
TRINITY_DN30467_c1_g1	<i>PIF3</i>	Forward (5'-3')	TGCTCTATACTTTCGCCGACCTT
		Reverse (5'-3')	CGACCCAAATAACAATACCCACC
TRINITY_DN26230_c0_g2	<i>MMK1</i>	Forward (5'-3')	CTATTCCTGTCCCGTTCTCCCTCTC
		Reverse (5'-3')	AGTAGCCTCCGTCATCACTGTATCG
TRINITY_DN30834_c0_g2	<i>AHK4</i>	Forward (5'-3')	GCCACGAGACAGATAAGGCAGAT
		Reverse (5'-3')	GGAGACATAACCATCCATCCCAC
TRINITY_DN29346_c1_g1	<i>AHK5</i>	Forward (5'-3')	GCTAATGCTGTTTCGCCTTCTCAATG
		Reverse (5'-3')	TTCCTCAAACCGATGCTCTTCCAAG

Experimental design and data analyses

All experiments and analyses were repeated three times. SPSS 26 was used for variance analysis and mean comparison ($P < 0.05$). (SPSS Inc. Chicago, USA).

Results and Discussions

Comparison of *S. chinensis* regenerated plant rooting under dark and light conditions

Light is the primary energy source for plant growth and is a complex environmental factor. To explore the effects of light and dark on the rooting of *S. chinensis* regenerated plants, we first determined the growth status, rooting rate, and germination rate of somatic embryos. As shown in Table 2, the embryogenic calli of *S.*

chinensis that were treated with light for 14 days underwent rapid expansion, and some of the somatic embryos exhibited green pigmentation. The somatic embryos that were exposed to light for 28 days displayed delicate, red hypocotyls. Conversely, after 14 days of dark treatment, most of the somatic embryos subjected to this darkness treatment expanded and elongated, while those treated with dark for 28 days exhibited thicker, well-grown, pale yellow hypocotyls. The rooting and germination rates were markedly higher under dark conditions than under light conditions (Fig. 1).

In plant tissue culture, light plays a crucial role in the proliferation and differentiation of culture materials, a development known as morphological plasticity, as a form of adaptation. Previous studies have shown that the natural development process of zygotic embryos occurs in a dark and relatively closed environment, suggesting that the induction and proliferation of somatic embryos may also require continuous dark or low light conditions (Wei 2017). Recent research demonstrated that short-term dark treatment significantly increased the germination rate of somatic embryos in *Paeifloria lactiflora* (Liu 2020). Similarly, dark treatment is also needed for embryogenic callus induction in the pedicel (Yu 2020). Zhou (2008) found that inducing embryogenic callus of peony in full darkness was more conducive to the induction of embryogenic cells and the formation of somatic embryos. In this study, somatic embryos of *S. chinensis* treated in the dark for 28 days showed a significantly higher rooting rate (95.56%) and germination rate (36.67%) than those treated with light, indicating that the dark environment is suitable for somatic embryo radicle development and indirectly promotes germination (Sun et al. 2013). These findings suggest that dark treatment can improve the rooting and germination rates of somatic embryos in various plant species.

Table 2
Effects of light and dark on the growth and development of somatic embryos in *S. chinensis*

Light condition	Rooting (%)	Germination (%)	Growth and development	
			14 d	28 d
Light	4.11 ^b	15.56 ^b	Some somatic embryos rapidly expanded and acquired a green color	The hypocotyl of germinating somatic embryos are predominantly slender and acquired a red color
Dark	95.56 ^a	36.67 ^a	Most somatic embryos undergo swelling and elongation	The hypocotyl of germinating somatic embryos appears pale yellow and exhibits increased thickness

Histological observation at different stages of somatic embryo development in *S. chinensis*

Histological analysis of somatic embryo development confirmed the period of occurrence and development of root primordia. The morphological characteristics of the *S. chinensis* somatic embryos cultured under dark or light conditions were observed at 7, 14, 21, and 28 days (Fig. 2). After the embryogenic calli (Fig. 2A) were inoculated in somatic embryo induction medium under dark conditions, radicle primordia developed during the globular embryo stage on day 7 (Fig. 2B), followed by development of the radicle during the heart-shaped embryo stage on day 14 (Fig. 2C). Subsequently, the radicle gradually elongated during the torpedo-shaped

embryo stage on day 21 (Fig. 2D) and fully developed during the cotyledon embryo stage on day 28 (Fig. 2E). In contrast, under light treatment, the majority of the *S. chinensis* somatic embryos failed to develop normally, with a large proportion of the embryos failing to form radicle primordia at the globular embryo stage (Fig. 2F). A few radicle primordia emerged at the heart-shaped embryo stage on day 14 (Fig. 2G) but did not develop and elongate during the torpedo-shaped embryo stage on day 21 (Fig. 2H). Most of the embryos remained in the torpedo-shaped embryo stage and gradually turned brown, possibly due to radicle primordium defects. Only a few of the embryos developed into cotyledon embryos on day 28 and formed complete plants (Fig. 2I).

Quantification of Endogenous Hormones during Somatic Embryogenesis of *S. chinensis*

The endogenous hormone content in plants has an important influence on plant organ morphogenesis. Here, we measured the endogenous hormone content in somatic embryo development under light and dark conditions. As shown in Fig. 3, the concentration of indole-3-acetic acid (IAA) was significantly higher in the light treatment ($597.565 \text{ ng}\cdot\text{g}^{-1}$) than in the dark treatment ($190.965 \text{ ng}\cdot\text{g}^{-1}$), exhibiting a threefold increase. Under dark culture conditions, the IAA content increased significantly during the torpedo-shaped embryo stage ($371.230 \text{ ng}\cdot\text{g}^{-1}$), potentially promoting radicle elongation. The abscisic acid (ABA) contents from the globular embryo stage to the heart-shaped embryo stage were higher under the light treatment ($749.188 \text{ ng}\cdot\text{g}^{-1}$ and $1019.859 \text{ ng}\cdot\text{g}^{-1}$) than under the dark treatment ($525.152 \text{ ng}\cdot\text{g}^{-1}$ and $824.755 \text{ ng}\cdot\text{g}^{-1}$) but lower at the torpedo-shaped embryo stage ($329.906 \text{ ng}\cdot\text{g}^{-1}$ and $629.372 \text{ ng}\cdot\text{g}^{-1}$). The gibberellic acid (GA_3) content was consistently higher under the dark treatment ($141.227 \text{ ng}\cdot\text{g}^{-1}$, $81.744 \text{ ng}\cdot\text{g}^{-1}$, $51.900 \text{ ng}\cdot\text{g}^{-1}$ and $48.676 \text{ ng}\cdot\text{g}^{-1}$) than under the light treatment ($245.153 \text{ ng}\cdot\text{g}^{-1}$, $176.713 \text{ ng}\cdot\text{g}^{-1}$, $61.460 \text{ ng}\cdot\text{g}^{-1}$ and $93.131 \text{ ng}\cdot\text{g}^{-1}$) during somatic embryo development, suggesting that dark treatment may enhance GA_3 content, thereby promoting further somatic embryo development and cotyledon embryo formation. The zeatin riboside (ZR) contents during the globular embryo stage, heart-shaped embryo stage, and cotyledon embryo stage were higher under the dark treatment ($1203.354 \text{ ng}\cdot\text{g}^{-1}$, $1173.912 \text{ ng}\cdot\text{g}^{-1}$, and $2328.489 \text{ ng}\cdot\text{g}^{-1}$) than under the light treatment ($2216.410 \text{ ng}\cdot\text{g}^{-1}$, $1595.285 \text{ ng}\cdot\text{g}^{-1}$, and $3497.238 \text{ ng}\cdot\text{g}^{-1}$), with both treatment groups exhibiting the lowest ZR value at the torpedo-shaped embryo stage and the highest value at the cotyledon embryo stage.

The synergistic or antagonistic effects of hormones regulate plant somatic embryo development, radicle development, and plant regeneration. In this study, the *S. chinensis* radicle primordium was initiated during the globular embryo stage and developed during the heart-shaped embryo stage. The IAA content during this period was lower under the dark treatment than under the light treatment. Under light treatment, the IAA content during the globular embryo period was up to 598.99 ng/g , which is similar to the IAA content in abnormal embryos of *S. chinensis* (Sun et al. 2013). We also observed that more deformed embryos were produced under light culture conditions, possibly due to the high concentration of auxin ($597.565 \text{ ng}\cdot\text{g}^{-1}$) caused by light in the early stage of somatic embryo development. The IAA content decreased to a normal level ($202.628 \text{ ng}\cdot\text{g}^{-1}$) during the heart-shaped embryo stage and induced root primordium formation. However, the IAA content increased sharply again during the torpedo-shaped embryo stage, which may have inhibited further radicle development. When there are defects in radicle development, somatic embryos cannot develop completely, resulting in gradual browning. Similar to our result, Yan et al. (2019) found that the highest IAA content was 112.44 ng/g during the rooting induction period of *Pyrus betulifolia* tissue culture seedlings. Therefore, we speculate that dark treatment may reduce the occurrence of abnormal embryos and that an

appropriate IAA concentration has a positive regulatory effect on somatic radicle production. Studies have shown that ABA may act as an endogenous signal to negatively regulate the role of IAA in promoting root formation during root morphogenesis (Eisner et al. 2021). Li et al. (2019) also showed that ABA negatively regulates IAA-related gene expression and affects rice root growth. In this study, the ABA level was lower under the dark treatment than under the light treatment from the globular embryo formation stage to the heart-shaped embryo stage. Therefore, we hypothesized that dark treatment reduces ABA levels from the globular embryo formation stage (7 d) to the heart-shaped embryo stage (14 d), weakening the negative regulatory effect of ABA on IAA and promoting the initiation of root primordia and the induction of radicles in *S. chinensis*.

Sequencing data and quality control

A total of 228.69 GB of raw sequence data were generated by sequencing samples of *S. chinensis* at each stage of the embryonic development cycle. Clean reads (194.03 GB) were obtained by filtering the sequence data using FastQC software. The quality control results are presented in Table 3. The total transcript count was 164,109, with a GC content of 42.70% (Fig. 4).

Table 3
List of data output quality

Sample	Raw_Reads	Raw_Bases	Valid_Reads	Valid_Bases	Valid%	Q20%	Q30%	GC%
CK	144605222	21.70G	141552600	19.77G	97.88	98.20	94.31	46.82
GZ1	140059378	21.00G	136838952	19.10G	97.66	98.11	94.10	46.97
GZ2	124945708	18.74G	122886202	17.16G	98.36	98.08	94.02	46.72
GZ3	134389322	20.16G	123980604	17.33G	92.20	98.21	94.31	46.90
GZ4	127168264	19.08G	122010946	17.04G	95.93	98.13	94.14	46.52
GZ5	143330914	21.50G	114968252	16.03G	79.71	98.09	94.06	46.72
HA1	130046422	19.51G	127297976	17.77G	97.89	98.08	93.99	46.89
HA2	150043174	22.51G	138540892	19.35G	92.28	98.13	94.14	47.09
HA3	142873138	21.44G	127014986	17.73G	88.90	98.10	94.09	47.10
HA4	132080040	19.81G	127228978	17.77G	96.63	98.27	94.54	46.96
HA5	154934928	23.24G	152011756	21.22G	98.13	98.10	94.08	47.06

Functional annotation and differential expression of Unigenes

As a complete genome sequence of *S. chinensis* is not available, in this study, the gene sequences that were obtained were compared with those in five publicly available databases: GO, KEGG, Pfam, Swissprot, eggNOG, and NR (Table 4). The results revealed that 21994 (35.11%), 17538 (28.00%), 20717 (33.88%), 18173 (29.00%),

25385 (40.53%), and 26794 (42.78%) genes were identified in the GO, KEGG, Pfam, Swissprot, eggNOG, and NR databases, respectively.

Table 4
Statistics of unigene annotation results

Database	Num	Ratio(%)
NR	26794	42.78
GO	21994	35.11
KEGG	17538	28.00
Pfam	20717	33.08
SwissProt	18173	29.01
eggNOG	25385	40.53
All	62636	100.00

The transcriptome data for the somatic embryos of *S. chinensis* under the two treatments were analyzed, revealing 3538 differentially expressed genes under dark conditions compared to light. The GO enrichment analysis (Fig. 5) showed that dark treatment enriched 733 GO terms, with biological process (BP) accounting for 60.66%. These included redox reduction, response to auxin and cytokinin, and cell wall organization. Cellular component (CC) and molecular function (MF) terms accounted for 12.02% and 27.32%, respectively. Most of the differentially expressed genes under the dark treatment were related to biological processes, including hormone and cell wall composition. The KEGG enrichment analysis (Fig. 6) allocated the differentially expressed genes to 20 pathways, with plant hormone signal transduction enriched in 264 genes, phenylpropanoid biosynthesis enriched in 63 genes, starch and sucrose metabolism enriched in 155 genes, circadian rhythm-plant enriched in 66 genes, and flavonoid biosynthesis enriched in 87 genes.

Plant hormone signal transduction pathway

In this study, the plant hormone signal transduction pathway revealed that dark treatment induced the responses of various hormones, including auxin, cytokinin, and gibberellin (Fig. 7). As one of the earliest discovered and most extensively studied plant hormones, auxin plays a crucial role in multiple stages of growth and development, such as plant embryogenesis, root development and elongation, and vascular tissue differentiation. In this study, the genes involved in auxin signal transduction and root development were *ARF*, *AUX/IAA*, etc. Compared to light culture conditions, under dark conditions, *ARF1* was significantly upregulated from the heart-shaped embryo stage to the cotyledon embryo stage, while *ARF2* and *AUX/IAA* were significantly upregulated from the globular embryo stage to the cotyledon embryo stage. *ARF18*, an auxin response factor, is a key factor that affects the downstream auxin transcription process, including activation or inhibition, to control changes in auxin content. In this study, *ARF18* was significantly upregulated from the heart-shaped embryo stage to the cotyledon-shaped embryo stage under light conditions. Phenotypic analysis of *OsARF18* transgenic materials showed that *OsARF18* could inhibit the elongation of rice roots (Xu 2021).

Aux/IAA (auxin/indole-3-acetic acid) is an early auxin response gene, and its protein product can specifically bind to *ARF*. The C-terminal domain CTD (C-terminal domain) of *ARF* is highly homologous to Domains III and IV of the *Aux/IAA* protein, which form dimers through these two regions to regulate the transcription of auxin response genes (Tiwari et al. 2003). Therefore, it is speculated that *ARF* and *Aux/IAA* effectively regulate the activity of auxin by specific binding under dark conditions, thus promoting radicle development.

Several key genes enriched in the cytokinin signal transduction pathway were identified, including type *B ARR*, *CRE1*, and *AHK5*. *CRE1*, a membrane-bound protein, acts as a negative regulator of cytokinin signal transduction (Kim et al. 2006), which is highly upregulated during the globular embryo stage under dark conditions. *B-ARR* plays a positive regulatory role in mediating CTK signal transduction by connecting IAA and CTK (Muller and Sheen 2007) and is significantly upregulated during each period of dark culture. *ARR1* can bind to the promoter of the negative regulator of the auxin signaling pathway *SHY2/IAA3* to activate gene expression, thereby regulating root development (Li et al. 2015). In this study, *ARR1* gene expression was downregulated under dark treatment and upregulated under light treatment. The downregulated expression of *CRE1* and the significantly upregulated expression of B-ARR in the dark environment may alter cytokinin content distribution. The combination of *ARR1* and auxin response factors also affects auxin level changes, regulating the formation and development of the radicle. *AHK5*, a cytokinin receptor (*Arabidopsis AHK4* histidine kinase), transmits cytokinin signals across the cell membrane, affecting endogenous cytokinin content.

MMK1, a downstream transcription factor of gibberellin, directly targets and binds to promoter elements of light signals and modulates the gibberellin content in somatic embryos. In this study, *MMK1* was upregulated under light treatment and negatively regulated radial growth. *PIF3*, a photosensitive interaction factor downstream of the photoreceptor, which is also a downstream transcription factor of the *DELLA* protein in the gibberellin pathway, negatively regulates auxin signaling. The downregulation of *PIF3* expression from the globular to torpedo-shaped embryo stages induced the downregulation of *AUX/IAA*, which in turn affected the upregulation of the cytokinin negative regulator *B-ARR* and negative regulator *CRE1*. *PIF3* is also a downstream transcription factor of the *DELLA* protein in the gibberellin pathway, indicating that the combined action of auxin, cytokinin signaling pathways, and gibberellin signal transduction promotes the development of somatic radicles in the later stage.

Circadian rhythm pathway

The KEGG enrichment analysis revealed that 66 genes were enriched in circadian rhythm pathways (Fig. 8), including photosensitive interaction transcription factor PIFs, cryptochrome *CRY1*, and downstream transcription factors *HY5* and *COP1*. Most genes in this pathway exhibited lower expression in the dark environment than in the light treatment, suggesting that these photoreceptors regulate the growth and development pattern of somatic embryos by up- or downregulating gene expression. *PIF3*, a downstream factor of the photoreceptor, negatively regulates auxin signaling and is also a downstream transcription factor of the *DELLA* protein in the gibberellin pathway. *PIF4* activates *IAA19* and *IAA29* by binding to the G-box (CACGTG) sequence in the promoter of auxin/indoleacetic acid genes, thereby regulating auxin and light signal transduction in plants (Kami et al. 2012). *COP1* has been shown to bind to *HY5* in the dark environment, leading to the inactivation or degradation of these transcription factors, and *HY5* can inhibit lateral root development (Jing and Lin 2017). Therefore, it is speculated that genes related to circadian rhythm that are

expressed in response to the dark environment may interact with hormone-related genes and participate in the formation and development of radicles in *S. chinensis*.

Phenylpropanoid biosynthesis pathway

During the initial phase of dark treatment, there was a significant increase in the expression of genes associated with phenylpropanoid synthesis (Fig. 9). A total of 63 differentially expressed genes were enriched in the phenylpropanoid biosynthesis pathway, including 17 cinnamyl alcohol dehydrogenase ELIs, 36 peroxidase PERs, and 10 shikimate hydroxycinnamoyl transferase SALATs. These findings suggest that *S. chinensis* somatic embryos produce numerous secondary metabolites in response to changes in environmental light conditions. Notably, peroxidases are the primary components that may influence or participate in the development of somatic embryos.

The phenylpropanoid biosynthesis pathway primarily generates lignin precursors, which are subsequently polymerized into lignin and incorporated into the cell wall (Scully et al. 2016). The transcriptome sequencing in this study revealed a significant enrichment of genes involved in the phenylpropanoid biosynthesis pathway, including peroxidase, cinnamate dehydrogenase (CAD), and cinnamyl coenzyme A reductase (CCR). Under chromium stress, upregulation of CCR and CAD genes has been found to result in increased wood deposition in the cell wall of two bean (*Vicia sativa* L.) cultivars (Rui et al. 2018). These findings suggest that genes encoding CCR, CAD, and peroxidase are involved in cell wall expansion by regulating lignin biosynthesis, particularly in vascular and fiber cells. As a result, they may play a role in regulating the development of *S. chinensis* radicles.

RT–qPCR analysis

Nine genes (*GH3*, *SAUR*, *ARF1*, *ARF18*, *AUX/IAA*, *MMK1*, *AHK4*, *AHK5* and *PIF3*) related to the plant hormone signal transduction pathway were chosen for RT–qPCR analysis. The qPCR analysis resulted in an expression pattern of target genes that was consistent with the transcriptome data under both light and dark cultivation conditions (Fig. 10), thereby affirming the accuracy of the transcriptome. The formation and development of the radicle in *S. chinensis* is a complex physiological process, and changes in light conditions may lead to up- or downregulation of these genes. The results suggest that the expression regulation of these nine genes plays a crucial role in modulating endogenous hormone content.

Conclusion

In this study, we explored the physiological and molecular mechanisms of dark conditions in promoting radicle development in *S. chinensis*. The rooting rate of *S. chinensis* somatic embryos was significantly higher (95.56%) under the dark treatment than under the light treatment. Paraffin section observations revealed that the radicle of *S. chinensis* was produced during the globular embryo stage and extended during the heart-shaped embryo stage under dark conditions. Conversely, most somatic embryos failed to generate root primordia or ceased development during the heart-shaped embryo stage under light treatment. During the early stages of somatic embryo development, lower concentrations of IAA and ABA facilitated radicle formation, while higher concentrations of GA₃ and ZR promoted somatic embryo root growth. Transcriptome sequencing and bioinformatics analysis revealed that differentially expressed genes under dark treatment were mainly

involved in plant hormone signal transduction, circadian rhythm, phenylpropanoid biosynthesis, and flavonoid synthesis pathways. Nine genes related to hormone signal transduction were validated, and their expression was consistent with transcriptional levels. These findings suggest that the regulation and expression of these genes play a crucial role in the formation and development of *S. chinensis* somatic embryo radicles.

Through transcriptome sequencing and bioinformatics analysis, we identified significant enrichment of differentially expressed genes in plant hormone signaling pathways, circadian rhythm, and phenylpropanoid biosynthesis pathways. The expression of nine genes associated with plant hormone signal transduction was verified using fluorescence quantitative real-time PCR (qRT-PCR), and the results were consistent with the transcription levels of the genes. We suggest that the root-specific expression of these genes may be useful in the genetic improvement of crop plants for various applications, such as improving rooting, vegetative propagation of reluctant woody plants, and scaling up the industrial culture of adventitious roots. Further analysis is needed to illustrate the mechanism by which these genes regulate radicle formation and development.

Declarations

Author contributions Dan Sun: Conceptualization, Data curation, Formal analysis, Investigation, Methodology, Writing – original draft, Writing – review & editing. Susu Zhang: Data curation, Formal analysis, Investigation. Jun Ai: Conceptualization, data curation, formal analysis, funding acquisition, investigation, methodology, resources. Zhenxing Wang: Conceptualization, Investigation, Methodology, Project administration. Guangli Shi: Investigation, Data curation, Formal analysis, Methodology. Jianhui Guo: Conceptualization, formal analysis, methodology. Xin Song: Investigation, Project administration. Meng Li and Yunqing Liu: Investigation, Formal analysis.

Conflict of interest The authors declare that they have no known competing financial interests or personal relationships that could have appeared to influence the work reported in this paper.

Data availability All data generated or analyzed during this study are included in this manuscript and are available from the corresponding author upon reasonable request.

Acknowledgments This work was supported by the Talent Introduction Fund of Jilin Agricultural University (grant number 0214–202022920) and the Research Project in the Jilin Provincial Science and Technology Department (grant number 20210204083YY). We thank LC-Bio Technology Co. Ltd. (Hangzhou, China) for transcriptome sequencing.

References

1. Ai J, Wang YP, Wang ZX, Sun D, Shi GL, Liu XY, Xu PL, Guo JH (2022) Chinese *Schisandra* germplasm resources. China Agricultural Publishing House
2. Ai J, Wang ZX, Qin HY (2012) Research status and prospect of *Schisandra chinensis* in China. J Northeast Agri Univ 43 (10): 14-20. <https://doi.org/10.3969/j.issn.1005-9369.2012.10.005>

3. Bai R, Zhang XJ, Li YL, Liu JP, Zhang, HB, Xiao WL, Pu JX, Sun HD, Zheng YT, Liu LX (2015) SJP-L-5, a novel small-molecule compound, inhibits HIV-1 infection by blocking viral DNA nuclear entry. *BMC Microbiol* 15, 274. <https://doi.org/10.1186/s12866-015-0605-3>
4. Buchfink B, Xie C, Huson DH (2015) Fast and sensitive protein alignment using diamond. *Nat Methods* 12(1), 59. <https://doi.org/10.1038/nmeth.3176>
5. Duclercq J, Sangwan-Norreel B, Catterou M, Sangwan RS (2011) De novo shoot organogenesis: from art to science. *Trends Plant Sci* 16(11): 597-606. <https://doi.org/10.1016/j.tplants.2011.08.004>
6. Eisner N, Maymon T, Sanchez EC, Bar-Zvi D, Brodsky S, Finkelstein R, Bar-Zvi D (2021) Phosphorylation of Serine 114 of the transcription factor ABSCISIC ACID INSENSITIVE 4 is essential for activity. *Plant Sci* 3(05): 1-10. <https://doi.org/10.1016/j.plantsci.2021.110847>
7. Fehér A (2015) Somatic embryogenesis-stress-induced remodeling of plant cell fate. *Biochim Biophys Acta* 1849(4): 385-402. <https://doi.org/10.1016/j.bbagr.2014.07.005>
8. Gyula P, Schäfer E, Nagy F (2003) Light perception and signalling in higher plants. *Curr Opin Plant Biol* 6(05): 446-452. [https://doi.org/10.1016/s1369-5266\(03\)00082-7](https://doi.org/10.1016/s1369-5266(03)00082-7)
9. Imaizumi T, Schultz TF, Harmon FG, Ho LA, Kay SA (2005) FKF1 F-box protein mediates cyclic degradation of a repressor of CONSTANS in *Arabidopsis*. *Science* 309(5732):293-7. <https://doi.org/10.1126/science.1110586>
10. Jing YJ, Lin RC (2017) Advances in plant light signal transduction in China. *Acta Bot Sin* 52(03): 257-270. <https://doi.org/10.11983/CBB16150>
11. Kami C, Hersch M, Trevisan M, Genoud, T, Hiltbrunner A, Bergmann S, Fankhauser C (2012) Nuclear phytochrome A signaling promotes phototropism in *Arabidopsis*. *The Plant Cell* 24(02): 566-576. <https://doi.org/10.1105/tpc.111.095083>
12. Kim HJ, Ryu H, Hong SH, Woo HR, Lim PO, Lee IC, Sheen J, Nam HG, Hwang I (2006) Cytokinin-mediated control of leaf longevity by AHK3 through phosphorylation of ARR2 in *Arabidopsis*. *PNAS* 103(03): 814-819. <https://doi.org/10.1073/pnas.0505150103>
13. Li FJ (2012) Grafting rapid propagation technology research *Schisandra chinensis*. Jilin Agricultural University
14. Li JT, Fan HY, Zhao QQ (2019) Regulation of abscisic acid on auxin synthesis and transport in rice roots. *J Xinyang Norm Univ (Natural Science Edition)* 32(01): 39-46. <https://doi.org/10.3969/j.issn.1003-0972.2019.01.007>
15. Li J, Liu ZH, Xiang FN (2015) Study on the role of cytokinin response regulators in mediating the growth and development of *Arabidopsis thaliana*. *Life sci* 27(04): 509-514. <https://doi.org/10.13376/j.cblls/2015066>
16. Liu J, Mu X, Liang J, Zhang J, Qiang T, Li H, Li B, Liu H, Zhang B (2022) Metabolic profiling on the analysis of different parts of *Schisandra chinensis* based on UPLC-QTOF-MS with comparative bioactivity assays. *Front Plant Sci* 13:970535
17. Liu XT (2020) Establishment of peony embryo regeneration system. Shenyang Agricultural University
18. Martin M (2011) Cutadapt removes adapter sequences from high-throughput sequencing reads. *EMBnet J* 17, 10-12. <https://doi.org/10.14806/EJ.17.1.200>

19. Mortazavi A, Williams BA, McCue K, Schaeffer L, Wold B (2008) Mapping and quantifying mammalian transcriptomes by RNA-Seq. *Nat Methods* 5(7):621-628. <https://doi.org/doi:10.1038/nmeth.1226>
20. Muller B, Sheen J (2007) Advances in cytokinin signaling. *Science* 318(5847): 68-9. <https://doi.org/doi:10.1126/science.1145461>
21. Patro R, Duggal G, Love MI, Irizarry RA, Kingsford C (2017) Salmon provides fast and bias-aware quantification of transcript expression. *Nat methods* 14(4), 417-419. <https://doi.org/10.1038/nmeth.4197>
22. Robinson MD, McCarthy DJ, Smyth GK (2010) EdgeR: a bioconductor package for differential expression analysis of digital gene expression data. *Bioinformatics* 26(1), 139-140. <https://doi.org/10.1093/bioinformatics/btp616>
23. Rui HY, Zhang XX, Shinwari KI, Zheng LQ, Shen ZG (2018) Comparative transcriptomic analysis of two *Vicia sativa* L. varieties with contrasting responses to cadmium stress reveals the important role of metal transporters in cadmium tolerance. *Plant Soil* 423(01): 241-255. <https://doi.org/10.1007/s11104-017-3501-9>
24. Scully ED, Gries T, Sarath G, Palmer NA, Baird L, Serapiglia MJ, Dien BS, Boateng AA, Ge Z, Funnell-Harris DL, Twigg P, Clemente TE, Sattler SE (2016) Overexpression of SbMyb60 impacts phenylpropanoid biosynthesis and alters secondary cell wall composition in *Sorghum bicolor*. *Plant J: for cell and molecular biology* 85(3), 378-395. <https://doi.org/10.1111/tpj.13112>
25. Song Y, Shan B, Zeng S, Zhang J, Jin C, Liao Z, Wang T, Zeng Q, He H, Wei F, Ai Z, Su D (2021) Raw and wine processed *Schisandra chinensis* attenuate anxiety like behavior via modulating gut microbiota and lipid metabolism pathway. *J Ethnopharmacol* 266, 113426. <https://doi.org/10.1016/j.jep.2020.113426>
26. Sun D, Li HB, Li Q, Piao ZY (2013) Dynamic changes of endogenous IAA, ABA and GA 3 contents during somatic embryogenesis of *Schisandra chinensis*. *Acta Phytophysiol Sinica* 49(01): 70-74. <https://doi.org/10.13592/j.cnki.ppj.2013.01.008>.
27. Wang ZZ (2010) Study on the mechanism of underground transverse stalk of *Schisandra chinensis*. Chinese Academy of Agricultural Sciences
28. Wei DX (2017) Study on somatic embryo induction and callus redifferentiation of *Paeonia lactiflora*. Beijing Forestry University
29. Xu FG (2021) The mechanism of OsARF18 regulating rice root development and phosphorus uptake. Henan Agricultural University
30. Xu ZH, Zhang XS, Su YH, Hu YX, Xu L, Wang JW (2019) Plant cell totipotency and regeneration. *Sci China Life Sci* 49(10): 1282-1300
31. Yan S, Zhang SY, Xu K, Yuan JC, Li XG, Zhou JT, Cheng CG, Zhao DY (2019) Changes of polyamines, endogenous hormones and related oxidase activities in the rooting process of *Pyrus betulaefolia*. *J Fruit Sci* 36(03): 318-326. <https://doi.org/10.13925/j.cnki.gsxb.20180372>
32. Yu B, Huang LL, Zhu Y, Zhu GF, Sun YB (2020) Embryogenic callus induction and efficient plant regeneration of young pedicel of *Hippeastrum vittatum*. *Acta Hort Sinica* 47(05): 907-915. <https://doi.org/10.16420/j.issn.0513-353x.2019-0672>
33. Yuan S, Jia YJ, Lin HH (2003) Several physiological factors inducing plant somatic embryogenesis. *Plant Physiol Comm* 39(05): 508-512. <https://doi.org/10.13592/j.cnki.ppj.2003.05.041>

Figures

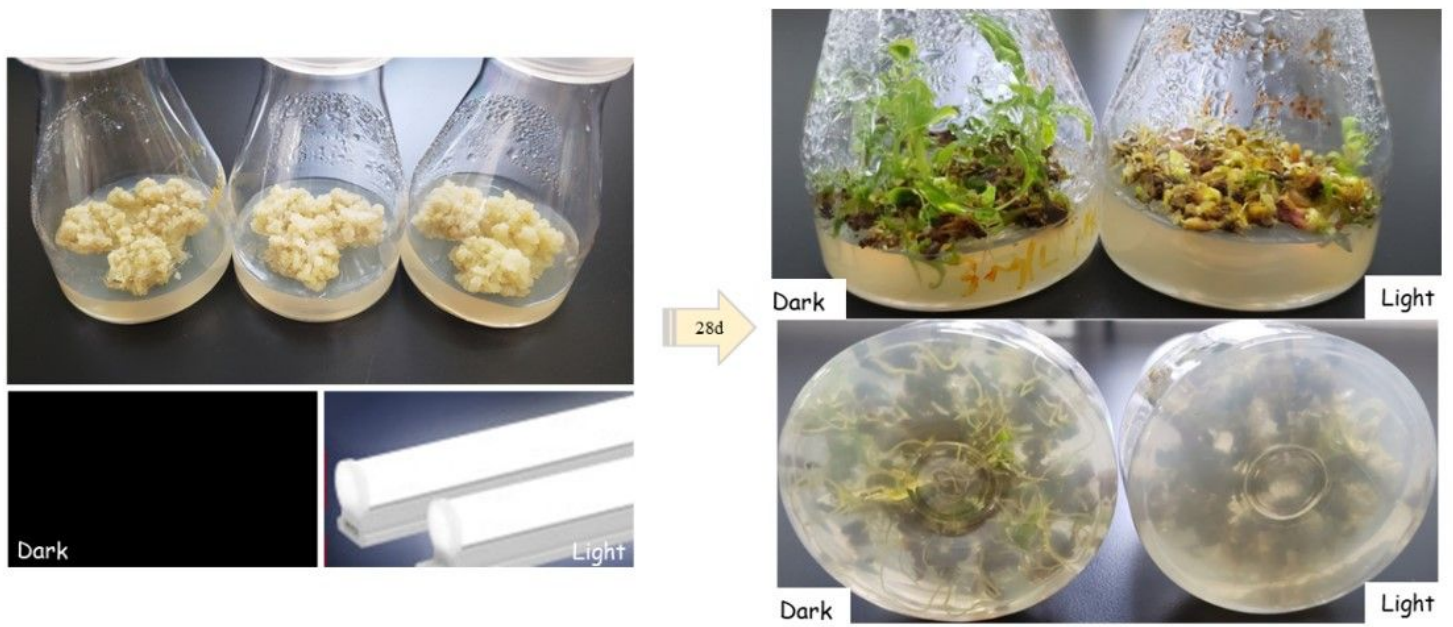


Figure 1

Growth and development of regenerated *S. chinensis* plantlets under light and dark conditions

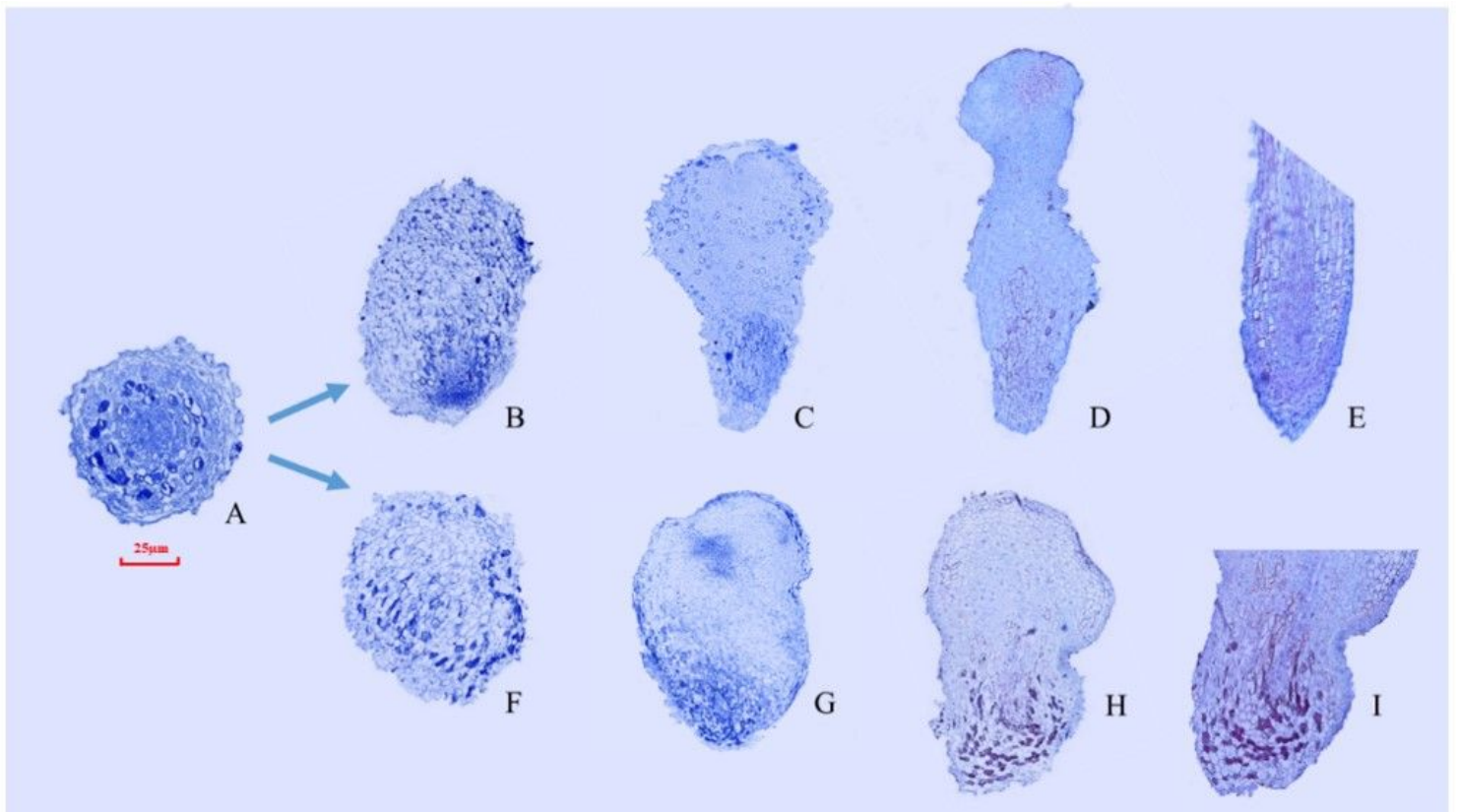


Figure 2

Development stages of somatic embryos in *S. chinensis* under different light conditions

A: Proembryo; B-E: Globular, heart-shaped, torpedo-shaped, and cotyledon-shaped embryo with radicle development under dark conditions; F-I: Globular, heart-shaped, torpedo-shaped, and cotyledon-shaped embryo with radicle development under light conditions.

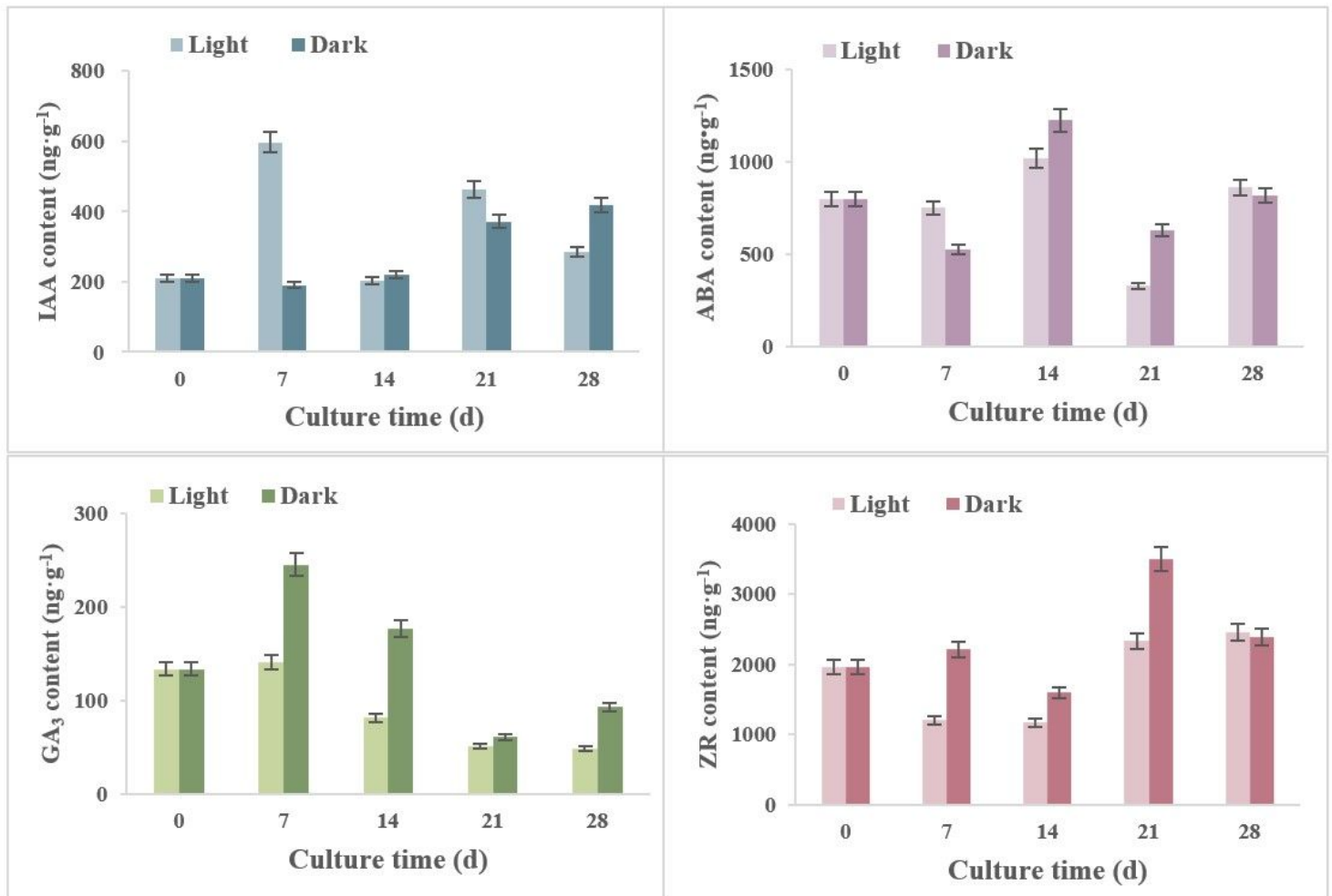


Figure 3

Changes in endogenous hormone levels during *S. chinensis* somatic embryogenesis under light and dark conditions.

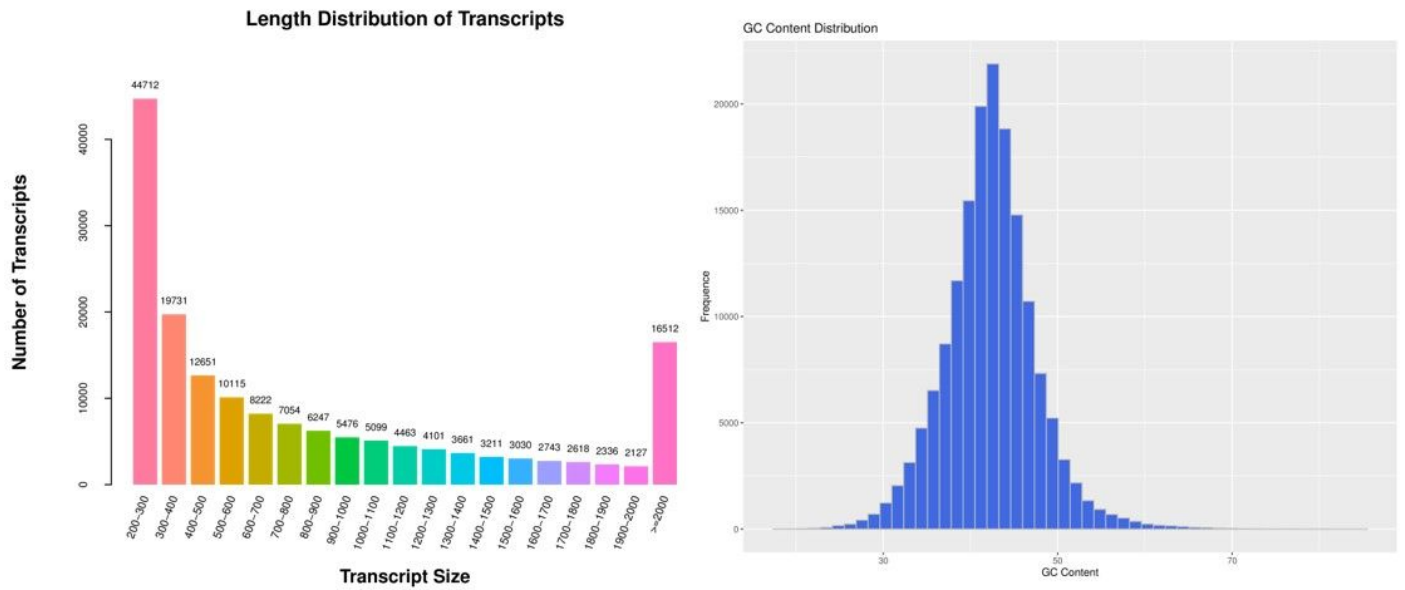


Figure 4

Length distribution of transcripts and GC content distribution

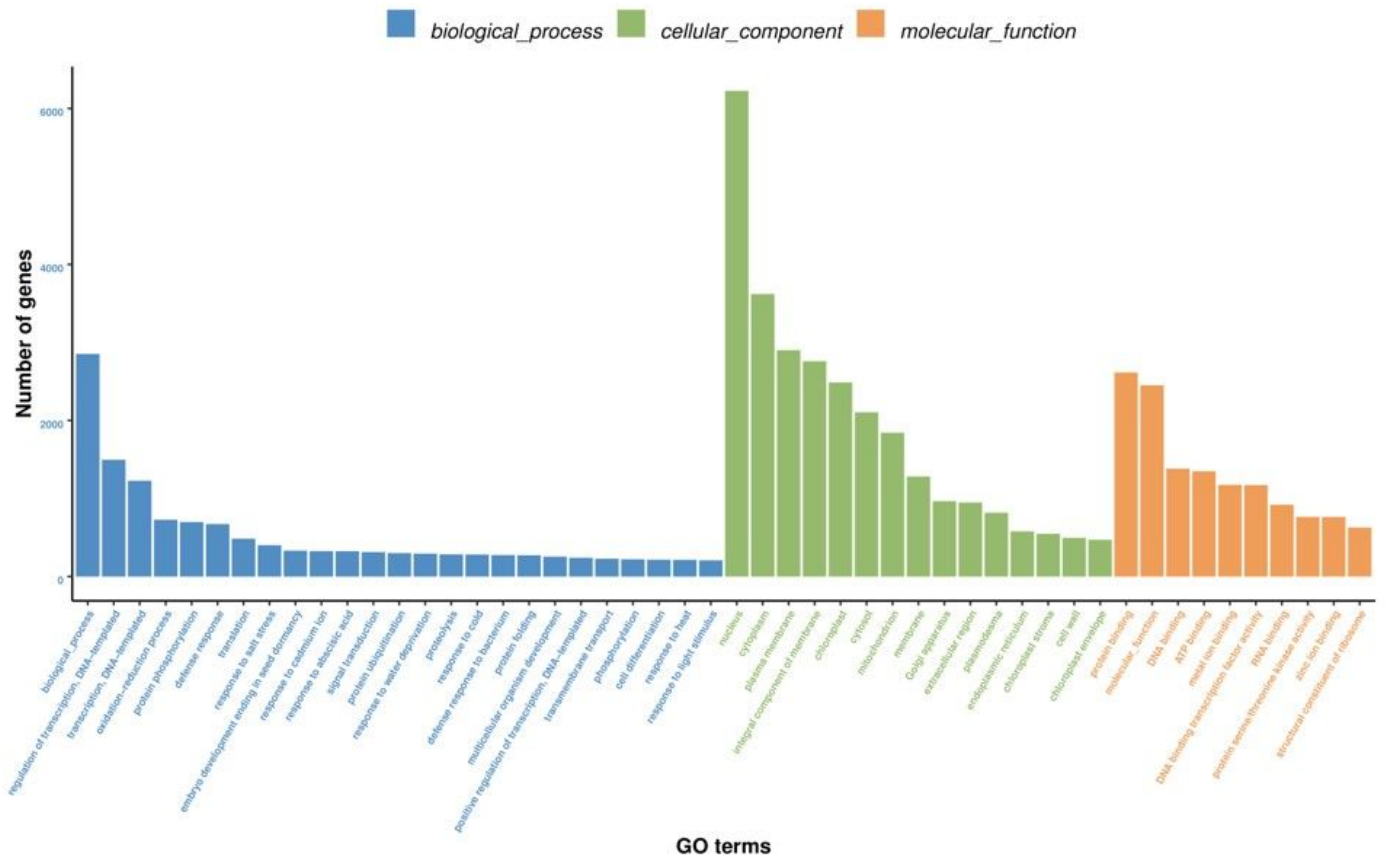


Figure 5

GO enrichment analysis of DEGs

KEGG Enrichment ScatterPlot

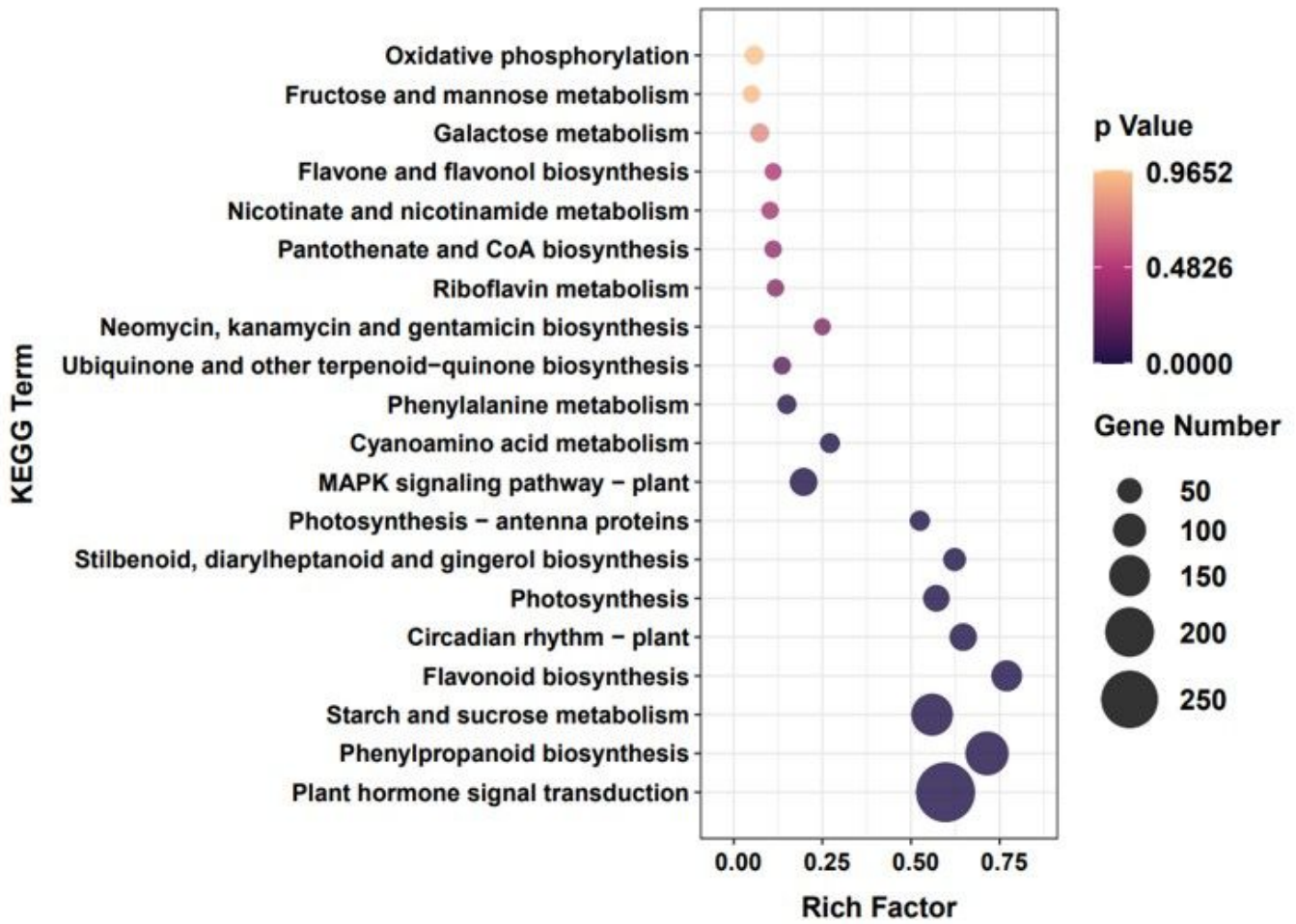


Figure 6

KEGG functional classification of differentially expressed genes

PLANT HORMONE SIGNAL TRANSDUCTION

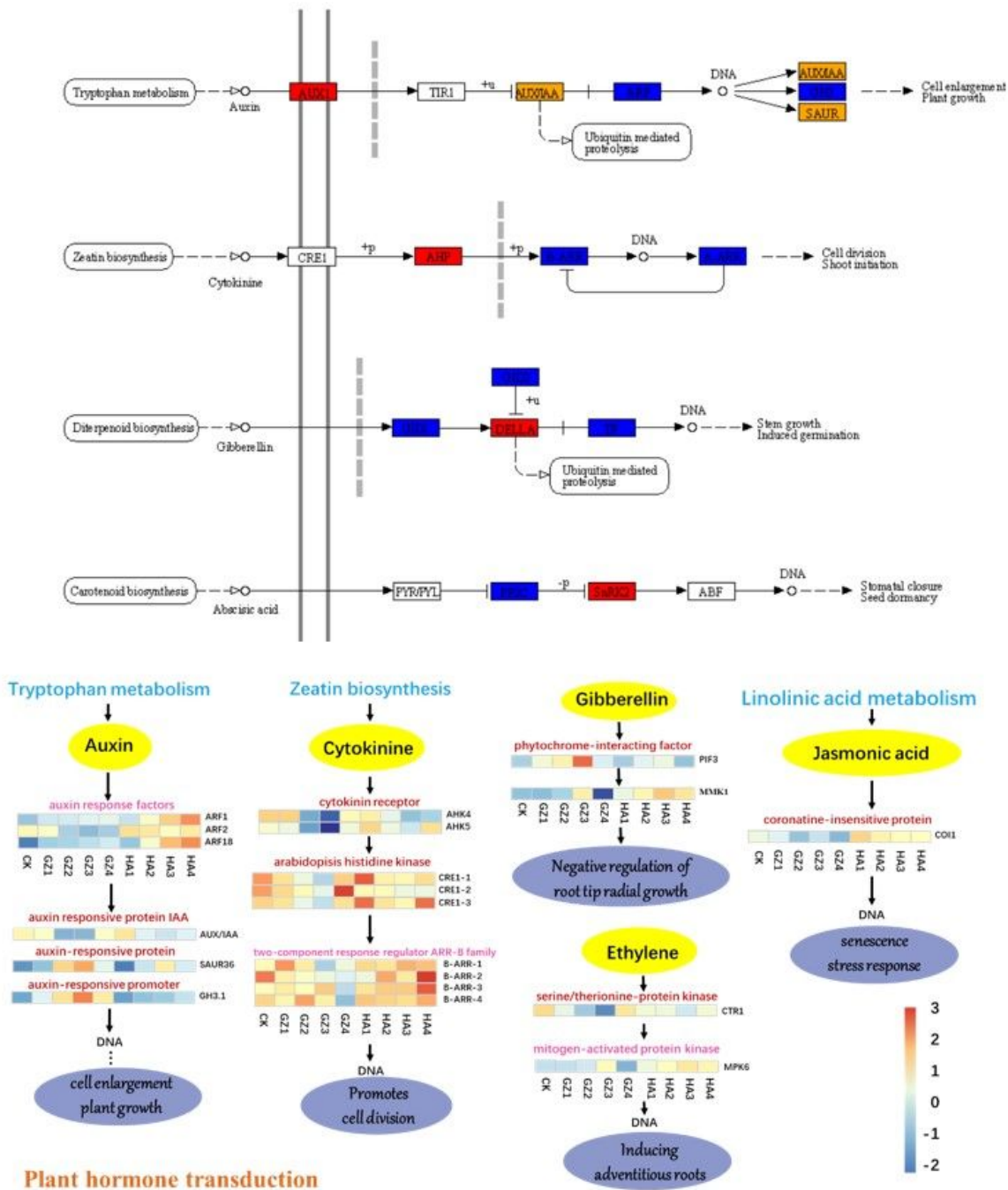
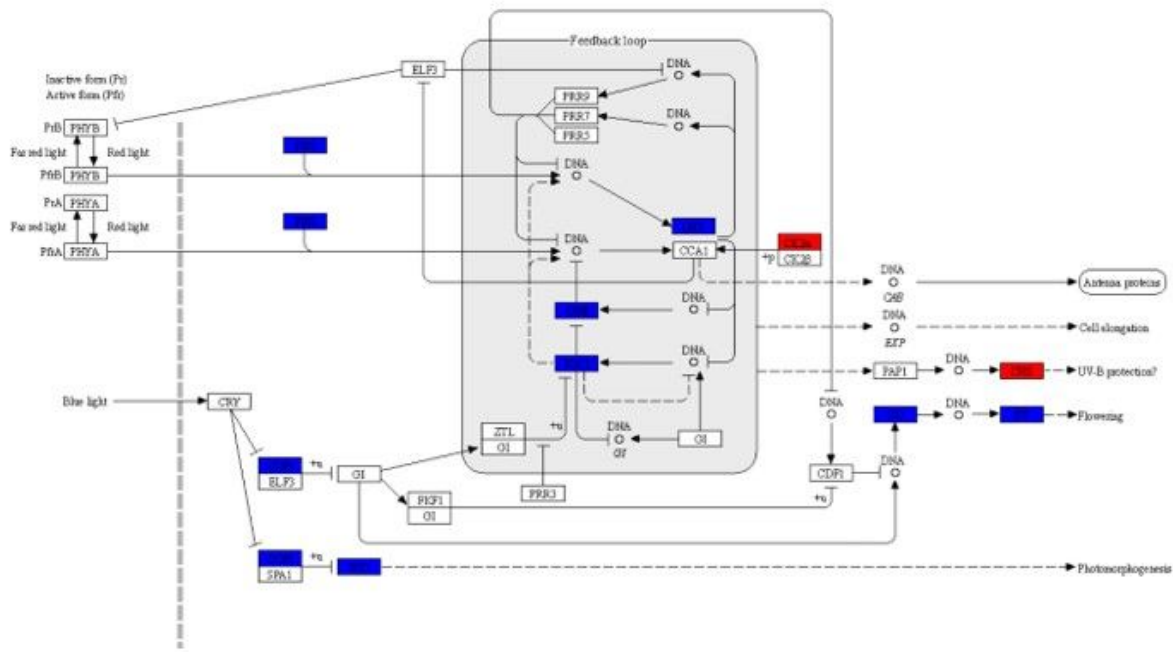


Figure 7

Differentially expressed genes in plant hormone signaling pathways.

The yellow ellipse represents the hormone, while the red and pink fonts indicate the downstream factors. The blue ellipses represent the metabolic processes.



circadian-rhythm plant

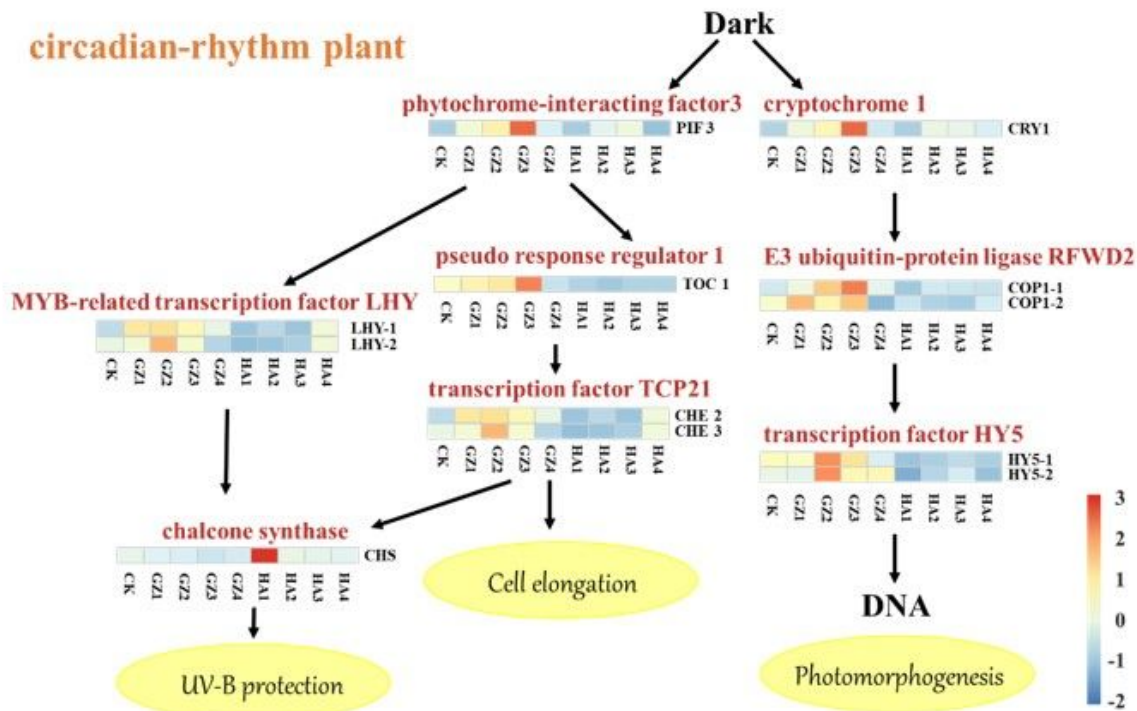


Figure 8

Differentially expressed genes involved in the circadian rhythm pathway

The downstream factors are highlighted in red font, while the yellow ellipses represent metabolic processes.

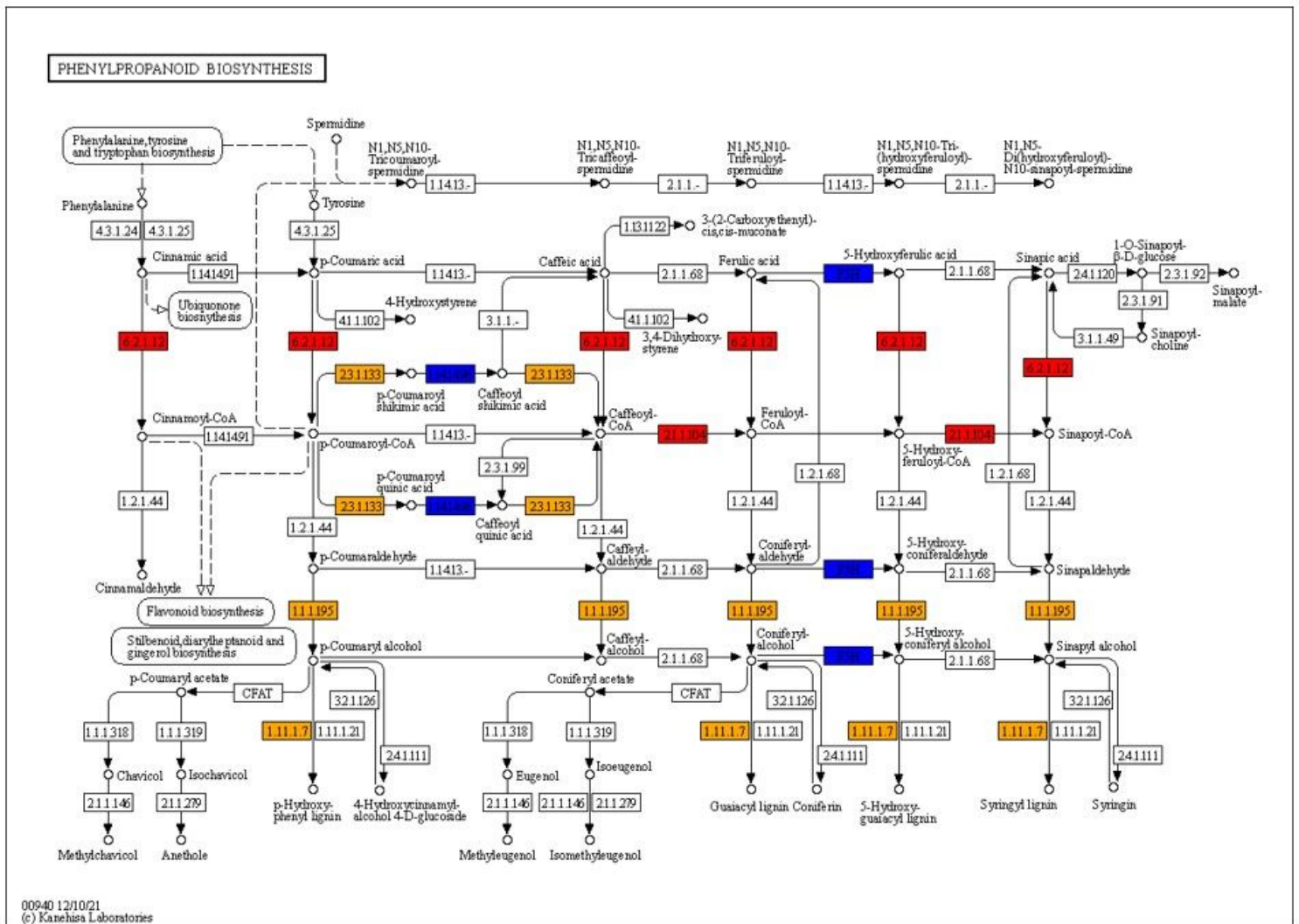


Figure 9

Differentially expressed genes in the phenylpropane biosynthesis pathway

The red box denotes upregulated expression, the blue box denotes downregulated expression, and the yellow box denotes both up- and downregulated expression.

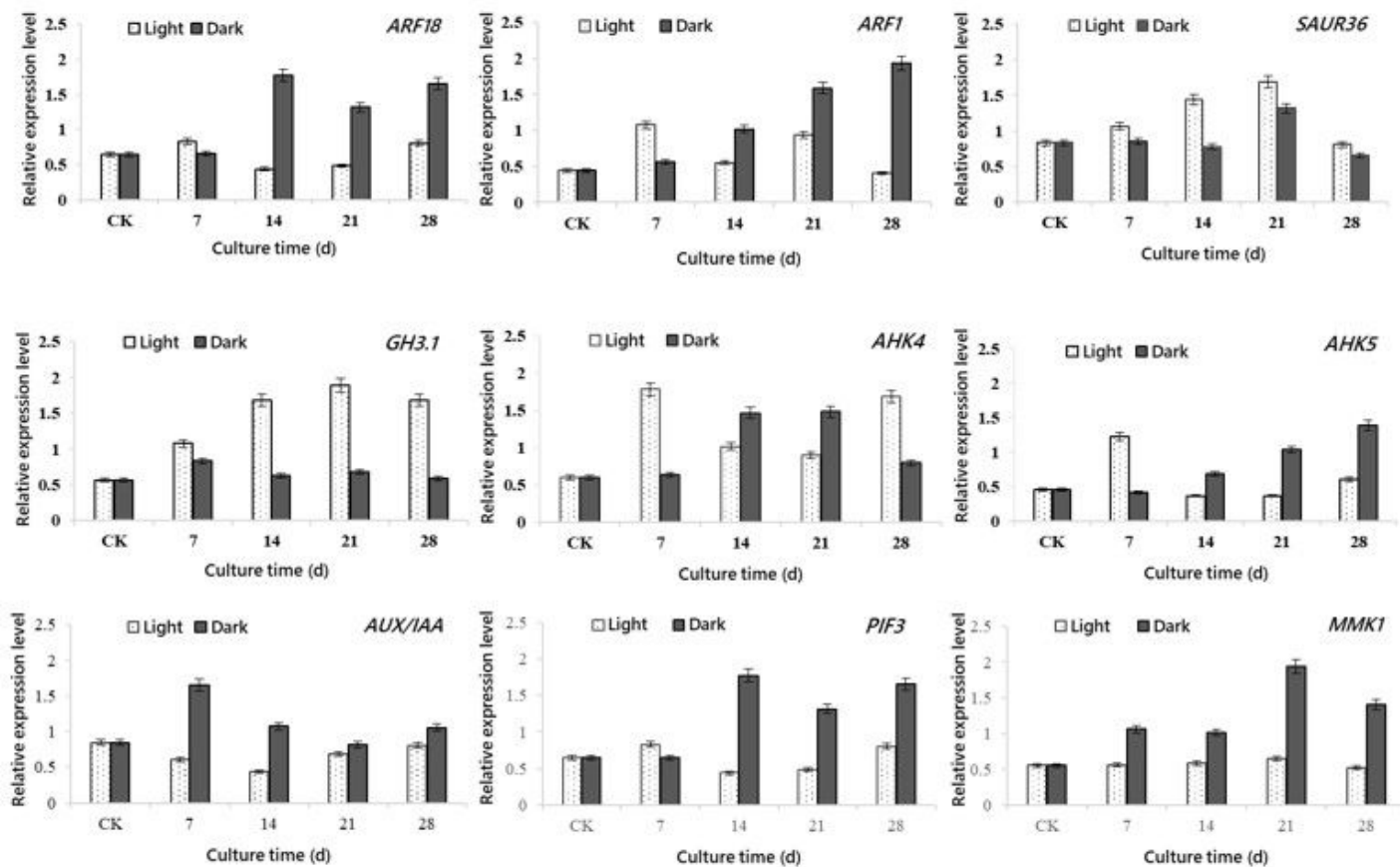


Figure 10

qRT-PCR validation of nine differentially expressed genes related to the plant hormone signal transduction pathway